J. Fluid Mech. (1998), *vol.* 370, *pp.* 1–27. Printed in the United Kingdom

On stagnation points and streamline topology in vortex flows

By HASSAN AREF[1] AND MORTEN BRØNS[2]

[1] Department of Theoretical and Applied Mechanics, University of Illinois, Urbana, IL 61801, USA

[2] Department of Mathematics, Technical University of Denmark, DK-2800 Lyngby, Denmark

(Received 11 March 1997 and in revised form 17 February 1998)

The problem of locating stagnation points in the flow produced by a system of N interacting point vortices in two dimensions is considered. The general solution follows from an 1864 theorem by Siebeck, that the stagnation points are the foci of a certain plane curve of class $N-1$ that has all lines connecting vortices pairwise as tangents. The case $N = 3$, for which Siebeck's curve is a conic, is considered in some detail. It is shown that the classification of the type of conic coincides with the known classification of regimes of motion for the three vortices. A similarity result for the triangular coordinates of the stagnation point in a flow produced by three vortices with sum of strengths zero is found. Using topological arguments the distinct streamline patterns for flow about three vortices are also determined. Partial results are given for two special sets of vortex strengths on the changes between these patterns as the motion evolves. The analysis requires a number of unfamiliar mathematical tools which are explained.

1. Introduction

There appear to be relatively few general results on the number, location and motion of stagnation points even in simple flows. Here we consider the stagnation points in two-dimensional flow on the unbounded plane produced by a system of N point vortices of arbitrary circulations.

It is well known that for point vortices the centre of vorticity remains fixed in time. A similar result holds for any vorticity distribution: If $\zeta(x, y, t)$ is the vorticity in two-dimensional ideal flow, the linear impulse,

$$\boldsymbol{P} = \iint \zeta \boldsymbol{x}\, \mathrm{d}\boldsymbol{x}, \tag{1.1}$$

is conserved (cf. Lamb 1932). If the total vorticity is non-zero, this leads to the invariance of the centroid of the vorticity distribution:

$$\boldsymbol{X} = \iint \zeta \boldsymbol{x}\, \mathrm{d}\boldsymbol{x} \Big/ \iint \zeta\, \mathrm{d}\boldsymbol{x}. \tag{1.2}$$

This invariance might lead one to believe that a fluid particle placed at $\boldsymbol{X}$ will remain stationary, in other words that there is always a stagnation point of the flow at $\boldsymbol{X}$. For certain simple cases, such as the motion of two identical vortices, this is true and follows from symmetry considerations. However, in general $\boldsymbol{X}$ is not a stagnation point.

Consider two point vortices of unequal circulations, Γ_1, Γ_2, and positions z_1, z_2 in the complex $z = x+\mathrm{i}y$ plane. The equations of motion for the vortices are

$$\frac{\mathrm{d}\bar{z}_1}{\mathrm{d}t} = \frac{1}{2\pi\mathrm{i}}\frac{\Gamma_2}{z_1-z_2}; \quad \frac{\mathrm{d}\bar{z}_2}{\mathrm{d}t} = \frac{1}{2\pi\mathrm{i}}\frac{\Gamma_1}{z_2-z_1} \tag{1.3}$$

(here and in the following overbars denote complex conjugation). It follows from (1.3), as a special case of (1.2), that the centre of vorticity,

$$z_V = \frac{\Gamma_1 z_1+\Gamma_2 z_2}{\Gamma_1+\Gamma_2}, \tag{1.4}$$

is constant in time. The fluid velocity (u, v) at z_V is given by

$$u-\mathrm{i}v = \frac{1}{2\pi\mathrm{i}}\left(\frac{\Gamma_1}{z_V-z_1}+\frac{\Gamma_2}{z_V-z_2}\right) = \frac{(\Gamma_2-\Gamma_1)(\Gamma_2+\Gamma_1)^2}{2\pi\mathrm{i}\Gamma_1\Gamma_2}\frac{1}{z_1-z_2}, \tag{1.5}$$

from which we see that only in the case $\Gamma_1 = \Gamma_2$ will z_V be a stagnation point.

A stagnation point, z_S, in the flow must satisfy the equation

$$\frac{\Gamma_1}{z_S-z_1}+\frac{\Gamma_2}{z_S-z_2} = 0, \tag{1.6}$$

i.e. be given by

$$z_S = \frac{\Gamma_1 z_2+\Gamma_2 z_1}{\Gamma_1+\Gamma_2} \tag{1.7}$$

(which should be read to imply that there is no finite stagnation point for $\Gamma_1 = -\Gamma_2$).

Consider the geometrical midpoint of the line segment joining vortices 1 and 2:

$$z_M = \tfrac{1}{2}(z_1+z_2). \tag{1.8}$$

We have

$$z_M = \tfrac{1}{2}(z_S+z_V). \tag{1.9}$$

Hence, *the stagnation point and the centre of vorticity are symmetrically placed with respect to the midpoint of the line joining the vortices*. It follows from this that the stagnation point moves in a circle about the centre of vorticity, as do the two vortices.

Although this example is entirely elementary, it serves to sensitize us to the problem at hand. Stagnation points are important for the understanding of advection of a passive scalar by the flow, and in the case of distributed vortices even for the dynamical evolution of the flow itself. Any information that we can obtain about their number, location and motion is very worthwhile.

In this paper we study one of the simplest cases – the flow due to an assembly of point vortices of arbitrary circulations. Even with this restriction a considerable amount of work must be done before results of any generality emerge. For point vortices the problem of locating stagnation points reduces to finding the roots of a certain polynomial. In practical terms finding such roots at any instant in time by numerical calculation is not a particularly difficult problem, at least not for moderate N. However, our objective is to derive general results, valid as the motion unfolds, and to understand the parametric dependence of the number, nature and location of stagnation points as the vortex circulations are varied. We state the problem in §2, and deduce a first, simple result. In §§3–4 we explain and explore a geometrical characterization of stagnation points as the foci of a certain curve. These developments

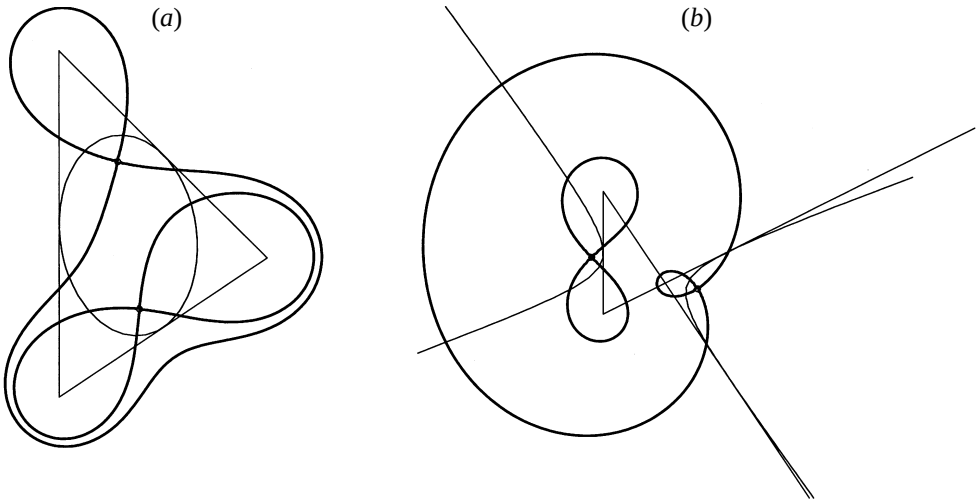

FIGURE 1. Three vortices, Siebeck curve, and separatrix streamlines of the flow. (*a*) Identical vortices (Siebeck's curve is an ellipse); (*b*) vortices of circulation 2, 2, -1 (Siebeck's curve is a hyperbola).

arise from geometrical theorems of Julius Plücker and his followers, notably an 1864 theorem by Siebeck. Because of the use of less familiar mathematical concepts, such as the complex projective plane, we devote §3 to a brief 'tutorial' on background material that is needed for Siebeck's theorem. In §4 we return to vortex dynamics and explore the case of flow due to three vortices on the unbounded plane in some detail. In §5 we take up a complementary approach in which we classify the pattern of streamlines in the flow about the three vortices using topological arguments. This approach is independent of the projective geometry of §§2–4. Taken together the results of the earlier sections on stagnation points and of §5 on streamline topology give the most comprehensive results on the flow pattern about a system of vortices that we have been able to find.

Figure 1 illustrates the inter-relation of the two thrusts of our analysis. In (*a*) we show three identical vortices, at some instant located at the vertices of the triangle shown. Inscribed in this triangle is an ellipse, which is the curve that arises in Siebeck's theorem for this case. The two foci of this ellipse are the stagnation points of the flow field produced by the three vortices. These aspects of figure 1(*a*) illustrate the developments through §4 below. Also shown is the pattern of instantaneous streamlines of the flow. The topology of this streamline pattern is one of the 12 determined in §5 (see figure 6a). The stagnation points are self-intersection points for the streamlines. In the last part of §5 we give results on the changes in streamline topology that occur as the motion of the vortices unfolds. A complete solution of this bifurcation problem for arbitrary vortex strengths is quite involved, and is not accomplished in this paper.

Figure 1(*b*) gives a similar diagram for the case of three vortices with circulations $\Gamma_1:\Gamma_2:\Gamma_3 = 2:2:(-1)$. Siebeck's curve for this case is a hyperbola that has all three sides of the vortex triangle as tangents. The stagnation points of the flow are the two foci of this hyperbola. Also shown in figure 1(*b*) are the separatrix streamlines, which form the pattern shown in figure 6(*c*).

For the case of three identical vortices the inscribed ellipse with foci at the stagnation points of the flow is known in geometry as the *Steiner ellipse*, and may be approached in a more elementary way than through the general theory. We refer the reader to

Schoenberg's (1982) book (in particular Chap. 7, §4). Schoenberg quotes and proves an 1888 theorem by van den Berg (which is a special case of Siebeck's theorem) for this case.

The strongest result we have obtained is for the case of three vortices of zero total strength. There is just a single stagnation point in this case, and we have found a 'similarity law' for its location.

In §6 we make some remarks on extensions of the methodology pursued here and state our main conclusions.

A preliminary account of this work was presented at the Forty-eighth Annual Meeting of the American Physical Society, Division of Fluid Dynamics, in Irvine, CA (Aref & Brøns 1995).

2. The general problem

Since the velocity (u, v) induced by a system of N point vortices is of the form

$$u - \mathrm{i}v = \frac{1}{2\pi\mathrm{i}} \sum_{\alpha=1}^{N} \frac{\Gamma_\alpha}{z - z_\alpha}, \tag{2.1}$$

it follows that the stagnation points are the roots of the polynomial

$$\begin{aligned} P(z) = {} & \Gamma_1(z-z_2)(z-z_3)\dots(z-z_N) \\ & + \Gamma_2(z-z_1)(z-z_3)\dots(z-z_N) + \dots \\ & + \Gamma_N(z-z_1)(z-z_2)\dots(z-z_{N-1}). \end{aligned} \tag{2.2}$$

Expanding this in powers of z, the leading terms are

$$\begin{aligned} P(z) = {} & (\Gamma_1+\Gamma_2+\dots+\Gamma_N) z^{N-1} - (\Gamma_1 z_2 + \Gamma_1 z_3 + \dots + \Gamma_1 z_N + \Gamma_2 z_1 + \Gamma_2 z_3 \\ & + \dots + \Gamma_2 z_N + \dots + \Gamma_N z_1 + \Gamma_N z_2 + \dots + \Gamma_N z_{N-1}) z^{N-2} + \dots . \end{aligned} \tag{2.3}$$

Thus, if the sum of the vortex strengths does not vanish, there are $N-1$ roots of the polynomial, i.e. $N-1$ stagnation points (although some of these may, of course, coincide). When the sum of the vortex strengths vanishes, there are at most $N-2$ distinct stagnation points.

The coefficient of z^{N-2} in (2.3) may be written as

$$-(\Gamma_1+\Gamma_2+\dots+\Gamma_N) \sum_{\alpha=1}^{N} z_\alpha + \sum_{\alpha=1}^{N} \Gamma_\alpha z_\alpha = (\Gamma_1+\Gamma_2+\dots+\Gamma_N)(z_V - N z_M), \tag{2.4}$$

where z_M denotes the 'midpoint' or centroid of the positions, defined as

$$z_M = \frac{1}{N} \sum_{\alpha=1}^{N} z_\alpha, \tag{2.5}$$

and, when the sum of strengths is non-zero, the centre of vorticity, z_V, is the discrete vortex counterpart of (1.2):

$$z_V = \sum_{\alpha=1}^{N} \Gamma_\alpha z_\alpha \Big/ \sum_{\alpha=1}^{N} \Gamma_\alpha. \tag{2.6}$$

The case when both the sum of strengths and the total impulse (which appears as the numerator of (2.6)) vanish is special: in this case the coefficient of z^{N-2} is zero, and there are at most $N-3$ different stagnation points. We remark that the four-vortex

problem, which is in general non-integrable, is in fact integrable in this special case (Eckhardt & Aref 1988; Eckhardt 1988). There is then at most one stagnation point in the flow.

For the case of N vortices we may now write a generalization of (1.9). If we denote the stagnation points by $z_1^{(S)}, \ldots, z_{N-1}^{(S)}$, we have

$$P(z) = (\Gamma_1 + \Gamma_2 + \ldots + \Gamma_N)(z - z_1^{(S)}) \ldots (z - z_{N-1}^{(S)}). \tag{2.7}$$

Expanding and comparing coefficients to (2.3), we see that in general

$$N z_M - z_V = z_1^{(S)} + \ldots + z_{N-1}^{(S)} \tag{2.8}$$

which may be written

$$\sum_{n=1}^{N-1} (z_n^{(S)} - z_M) = z_M - z_V. \tag{2.9}$$

Thus, *the sum of the vectors from the midpoint to the stagnation points equals the vector from the centre of vorticity to the midpoint*. In particular, for identical vortices the midpoint and the centre of vorticity coincide, and the sum of the vectors from the midpoint to the stagnation points vanishes. For $N = 2$ (2.9) reduces to (1.9).

Returning to the polynomial $P(z)$ – in the form (2.2) – we see that the problem of locating the stagnation points of a flow induced by N point vortices is equivalent to the problem of finding the location in the complex plane of the roots of this polynomial. The problem of locating the roots of a polynomial given through its coefficients has spawned a large literature in mathematics, much of which will be unfamiliar. The monograph by Marden (1949) provides a useful starting point for pursuing this literature. We were surprised to find that there exists a precise geometrical characterization of the location of the stagnation points for a system of N vortices as the foci of a certain explicitly given curve of class $N-1$ (we shall explain the notion of the *class* of a curve in §3) in the plane. The main result goes back to a paper by F. H. Siebeck (1864). Siebeck's work is based on the geometry of Julius Plücker (1801–1868), and utilizes the complex projective plane. The result is re-stated and elaborated by several later authors. We found the account by Heawood (1906) to be one of the more useful. The present paper arose in large measure from our attempts to understand Siebeck's theorem and its potential utility in determining the stagnation points of a simple vortex flow.

Siebeck's theorem is one of the first results in Marden's book – it is stated and proved on pp. 9–12 – and is, in fact, related there to the problem of finding the stagnation points of a system of sources and sinks! While we might simply refer the reader to Marden (1949), we feel it is appropriate to provide a quick 'tutorial' on the geometry of the complex projective plane in order to introduce various concepts and establish our notation, state and prove the theorem, and then proceed to a more detailed study of special cases. The three-vortex problem, in particular, where the curves that arise in Siebeck's theorem are conic sections, deserves further elaboration. Our main contribution, then, is a detailed discussion of the location of stagnation points in the three-vortex problem, and the attendant changes in topology that occur in the streamline pattern as the vortices (and stagnation points) move. There are, as we shall see, interesting connections to the general classification of three-vortex motion given many years ago (Synge 1949; Aref 1979). For the case of three vortices with sum of strengths equal to zero, where we have a very detailed understanding of the motion due to the work of Rott (1989) and Aref (1989), we are led to a 'similarity law' for the single stagnation point, that would seem difficult to find without the formalism pursued here. In general we may say that the merit of Siebeck's theorem is the geometric

characterization of the stagnation points as a function of the vortex positions and strengths that it provides. In terms of actual calculation, the extraction of roots of a low-order polynomial is a relatively trivial procedure, and efficient, direct, numerical methods for solving this problem can easily be given. We elaborate on this statement in §6.

It should be stressed that the stagnation points covered by the developments in this paper are those situated away from the vortices themselves. These are always saddle points of the streamfunction. (Indeed, because these stagnation points occur in potential flow, the streamlines must self-intersect at 90° angles.) There are configurations in which a particular point vortex may remain stationary, and if one smoothed the point vortex to a (small) finite-area vortex, one could argue that the flow has a stagnation point at the position of the stationary vortex itself. Such stagnation points, which are generally elliptic points of the streamfunction, are not captured by the theory developed here.

3. The complex projective plane and Siebeck's theorem†

We consider the set of triples of complex numbers $(x_1, x_2, x_3) \neq (0, 0, 0)$, i.e. the set $\boldsymbol{C}^3\backslash\{(0, 0, 0)\}$. Two such triples, (x_1, x_2, x_3) and (y_1, y_2, y_3), are considered to be equivalent if there exists a complex number, c, such that $(x_1, x_2, x_3) = (cy_1, cy_2, cy_3)$, and the set of triples is hereby divided into equivalence classes. The set of equivalence classes constitutes the *complex projective plane* $\boldsymbol{P}^2$, the 'points' of which may, thus, be thought of as 'rays' in $\boldsymbol{C}^3\backslash\{(0, 0, 0)\}$. Computations in $\boldsymbol{P}^2$ are performed on representatives of the equivalence classes, so when we use terms such as 'the point (x_1, x_2, x_3)', we mean the equivalence class that contains (x_1, x_2, x_3). The equivalence of proportional triples implies that the only algebraic expressions that are meaningful are homogeneous in the coordinates, and thus that during calculations dropping a common factor is permitted. We shall often designate a coordinate triple (x_1, x_2, x_3) simply by the symbol $(\boldsymbol{x})$.

For any point in $\boldsymbol{P}^2$ corresponding to a triple (x_1, x_2, x_3) with $x_3 \neq 0$, there corresponds a unique 'point' $(x_1/x_3, x_2/x_3)$ in the set of complex pairs $\boldsymbol{C}^2$. Thus, $\boldsymbol{P}^2$ contains $\boldsymbol{C}^2$, but also has additional elements, viz. all those triples for which $x_3 = 0$. These points will be called *ideal elements* of $\boldsymbol{P}^2$ or *points at infinity*. The usual plane, $\boldsymbol{R}^2$, viewed either as the complex plane, $\boldsymbol{C}$, or as the set of real pairs, is contained within $\boldsymbol{C}^2$. In order to distinguish it from the projective plane, we shall refer to $\boldsymbol{R}^2$ as the *affine plane*. It will be useful to consider statements of analytical geometry in the affine plane – which is where our vortices and stagnation points ultimately reside – as statements about entities in $\boldsymbol{P}^2$, to perform various manipulations in $\boldsymbol{P}^2$, and then to interpret the results in the affine plane. We need next to familiarize ourselves with the geometry in $\boldsymbol{P}^2$, and to see how to translate results back and forth between $\boldsymbol{R}^2$ and $\boldsymbol{P}^2$.

3.1. *Lines*

In $\boldsymbol{R}^2$ a line is given by an expression of the form

$$ax + by + c = 0, \tag{3.1}$$

† The mathematical apparatus developed here was treated by numerous authors in texts on algebraic geometry of the last century, e.g. Salmon (1854), Ferrers (1866). These treatments are, in principle, elementary, yet often appear rather inaccessible. Modern treatments, on the other hand, are often phrased in such general mathematical terms as to be difficult to use for purposes of practical calculation. An important exception is Chap. 12 of the book by Coxeter (1993), where much of the classical material is summarized using modern notation and point of view.

where x and y are the usual Cartesian coordinates of a variable point and a, b, c are certain numbers determining the line in question. Setting $x = x_1/x_3$, $y = x_2/x_3$, and multiplying through by x_3, we obtain an equation of the form

$$u_1 x_1 + u_2 x_2 + u_3 x_3 = 0 \tag{3.2a}$$

as the equation for a line in $\boldsymbol{P}^2$ (where x_1, x_2 and x_3 now are allowed to be complex). Note that this expression is, indeed, homogeneous in the coordinates. The points on the line are those triples (x_1, x_2, x_3) (as representatives of equivalence classes, as discussed above) for which the equation is satisfied. It is, therefore, natural to think of the triple $[u_1, u_2, u_3]$ as characterizing the line, and we call this triple the *coordinates of the line*. When we need to make the distinction, we will refer to (x_1, x_2, x_3) as the point coordinates (and use round brackets), and to $[u_1, u_2, u_3]$ as the line coordinates (and use square brackets). Note that $[u_1, u_2, u_3]$ is again determined only up to a constant of proportionality. Just as we may read (3.2*a*) as the equation of all the points (x_1, x_2, x_3) on the line $[u_1, u_2, u_3]$, we may also read it as the equation of all the lines $[u_1, u_2, u_3]$ passing through the point (x_1, x_2, x_3). In this way we begin to see the *duality* of points and lines in the formulation of geometry in the projective plane $\boldsymbol{P}^2$. All the ideal elements in $\boldsymbol{P}^2$ are on a line with coordinates [0, 0, 1], the *ideal line* or the *line at infinity*.

We shall often designate a triple of line coordinates $[u_1, u_2, u_3]$ simply by $[\boldsymbol{u}]$, and we shall use the convention of summing over repeated indices to write an equation such as (3.2*a*) in the form

$$u_i x_i = 0. \tag{3.2b}$$

Two different lines in $\boldsymbol{P}^2$ always intersect. To find the point of intersection of $[u_1, u_2, u_3]$ and $[v_1, v_2, v_3]$ we must solve the system

$$u_1 x_1 + u_2 x_2 + u_3 x_3 = 0, \tag{3.3a}$$

$$v_1 x_1 + v_2 x_2 + v_3 x_3 = 0. \tag{3.3b}$$

It is easily seen that the solution, up to a common factor, is

$$(x_1, x_2, x_3) = (u_2 v_3 - u_3 v_2, u_3 v_1 - u_1 v_3, u_1 v_2 - u_2 v_1), \tag{3.4}$$

and this is $\neq (0, 0, 0)$ unless $[u_1, u_2, u_3]$ and $[v_1, v_2, v_3]$ are proportional, i.e. so long as the lines are different. Two lines will intersect at an ideal point, i.e. $u_1 v_2 - u_2 v_1$ will vanish, precisely when the lines interpreted in $\boldsymbol{R}^2$ are parallel.†

Similarly, we may show that there is just one line through two different points $(\boldsymbol{x}) = (x_1, x_2, x_3)$ and $(\boldsymbol{y}) = (y_1, y_2, y_3)$. For this line, $[\boldsymbol{u}] = [u_1, u_2, u_3]$, must satisfy

$$u_1 x_1 + u_2 x_2 + u_3 x_3 = 0, \tag{3.5a}$$

$$u_1 y_1 + u_2 y_2 + u_3 y_3 = 0. \tag{3.5b}$$

Hence,

$$[u_1, u_2, u_3] = [x_2 y_3 - x_3 y_2, x_3 y_1 - x_1 y_3, x_1 y_2 - x_2 y_1], \tag{3.6}$$

and this is $\neq (0, 0, 0)$ unless $(\boldsymbol{x})$ and $(\boldsymbol{y})$ are proportional, i.e. unless they correspond to the same point in $\boldsymbol{P}^2$. We see the duality between a line through two points and a point at the intersection of two lines.

3.2. *General curves: order, class and tangents*

Let us consider a general algebraic curve $F(x_1, x_2, x_3) = 0$, where F is some homogeneous polynomial in its three variables. If F is of degree n, we say that the curve is of *order n*. A line in the projective plane will intersect a curve of order n at n points.

† We may also use the notation of vectors in three dimensions, e.g. by thinking of the incidence relation (3.2) as a 'scalar product' $\boldsymbol{u} \cdot \boldsymbol{x} = 0$, and the intersection of two lines $[\boldsymbol{u}]$ and $[\boldsymbol{v}]$ as being the point $(\boldsymbol{u} \times \boldsymbol{v})$. We show in (3.6) that the line connecting $(\boldsymbol{x})$ and $(\boldsymbol{y})$ is $[\boldsymbol{x} \times \boldsymbol{y}]$.

Using the homogeneity of F, namely, $F(\lambda x_1, \lambda x_2, \lambda x_3) = 0$ for any λ, we differentiate with respect to λ and set $\lambda = 1$ to obtain

$$\frac{\partial F}{\partial x_i} x_i = 0, \tag{3.7}$$

or, in 'vector notation', $\boldsymbol{x} \cdot \boldsymbol{\nabla} F = 0$.

On the other hand, the tangent to the curve at $(\boldsymbol{x})$ is the line connecting $(\boldsymbol{x})$ to an infinitesimally close point on the curve $(\boldsymbol{x} + \mathrm{d}\boldsymbol{x})$. This line is $[\boldsymbol{u}] = [\boldsymbol{x} \times \mathrm{d}\boldsymbol{x}]$. But $(\boldsymbol{x} + \mathrm{d}\boldsymbol{x})$ is also on the curve, so $F(\boldsymbol{x} + \mathrm{d}\boldsymbol{x}) = 0 = F(\boldsymbol{x}) + \mathrm{d}\boldsymbol{x} \cdot \boldsymbol{\nabla} F + \ldots$, or $\mathrm{d}\boldsymbol{x} \cdot \boldsymbol{\nabla} F = 0$. It follows from this and the preceding result, $\boldsymbol{x} \cdot \boldsymbol{\nabla} F = 0$, that $[\boldsymbol{x} \times \mathrm{d}\boldsymbol{x}] = [\boldsymbol{\nabla} F]$ (recall that a constant of proportionality may be dropped). Thus, the line $[\boldsymbol{u}] = [\boldsymbol{\nabla} F] = [\partial F / \partial \boldsymbol{x}]$ is the tangent to the curve at point $(\boldsymbol{x})$.

We may also consider an expression of the form $\Phi[u_1, u_2, u_3] = 0$, where Φ is some homogeneous polynomial in its three variables. The lines that satisfy this equation will in general have an envelope, which is a curve in the plane. If Φ is of degree m, we say that this curve is of *class m*. Through any point in the projective plane there will be m tangents to a curve of class m.

Again, by homogeneity

$$\frac{\partial \Phi}{\partial u_i} u_i = 0, \tag{3.8}$$

or $\boldsymbol{u} \cdot \boldsymbol{\nabla} \Phi = 0$.

A point on the curve, $(\boldsymbol{x})$, arises by finding the intersection of two infinitesimally close tangents $[\boldsymbol{u}]$ and $[\boldsymbol{u} + \mathrm{d}\boldsymbol{u}]$. The point of intersection of these two lines is $(\boldsymbol{x}) = (\boldsymbol{u} \times \mathrm{d}\boldsymbol{u})$. But $\Phi[\boldsymbol{u} + \mathrm{d}\boldsymbol{u}] = \Phi[\boldsymbol{u}] + \mathrm{d}\boldsymbol{u} \cdot \boldsymbol{\nabla} \Phi + \ldots = 0$, or $\mathrm{d}\boldsymbol{u} \cdot \boldsymbol{\nabla} \Phi = 0$. It follows from this and the preceding result, $\boldsymbol{u} \cdot \boldsymbol{\nabla} \Phi = 0$, that $(\boldsymbol{u} \times \mathrm{d}\boldsymbol{u}) = (\boldsymbol{\nabla} \Phi)$ (a constant of proportionality may again be dropped). Thus, $(\boldsymbol{x}) = (\boldsymbol{\nabla} \Phi) = (\partial \Phi / \partial \boldsymbol{u})$ is the point of tangency of the tangent $[\boldsymbol{u}]$.

The preceding considerations show us how to get the equation in line coordinates of a curve given in point coordinates and vice versa. Thus, to get the equation of the curve $\Phi[\boldsymbol{u}] = 0$ in point coordinates, write out the derivative, $\partial \Phi / \partial \boldsymbol{u}$, solve the three equations $\boldsymbol{x} = \partial \Phi / \partial \boldsymbol{u}$ for the u in terms of the x, and substitute the result into $\Phi[u_1, u_2, u_3] = 0$. Similarly, to get the equation of the curve $F(\boldsymbol{x}) = 0$ in line coordinates, write out the derivative, $\partial F / \partial \boldsymbol{x}$, solve the three equations $\boldsymbol{u} = \partial F / \partial \boldsymbol{x}$ for the x in terms of the u, and substitute the result into $F(x_1, x_2, x_3) = 0$.

3.3. *Conics*

A conic (or conic section) in $\boldsymbol{R}^2$ is given by a quadratic polynomial in the coordinates x and y. Again setting $x = x_1/x_3$, $y = x_2/x_3$, and multiplying through by x_3, we arrive at a homogeneous quadratic form in x_1, x_2, and x_3. We may write this *point conic* in $\boldsymbol{R}^2$ as

$$F(x_1, x_2, x_3) = a_{ij} x_i x_j = 0. \tag{3.9}$$

The conic is singular if the determinant of the symmetric coefficient matrix vanishes. It is in general *a curve of order* 2. In order to classify the conic we need to consider the sign of the determinant of the minor $\begin{bmatrix} a_{11} & a_{12} \\ a_{21} & a_{22} \end{bmatrix}$. The conic is an ellipse, parabola or hyperbola according to whether this determinant is positive, zero, or negative.

The tangent to the conic at $(\boldsymbol{x})$ is, according to §3.2, a line with coordinates

$$u_i = a_{ij} x_j. \tag{3.10}$$

If we solve these equations for the x in terms of the u, and then substitute the result into

$$u_1 x_1 + u_2 x_2 + u_3 x_3 = 0, \tag{3.11}$$

we obtain the equation of the conic in line coordinates:

$$\Phi[u_1, u_2, u_3] = \alpha_{ij} u_i u_j = 0, \tag{3.12}$$

where α_{ij} is the cofactor of a_{ij} in the determinant of the matrix $\{a_{ij}\}$. Thus, the conic is also *a curve of class* 2. In general, the order and the class of a curve are not identical. Plücker established general relations between order, class, and other characteristic numbers, such as the number of singularities on the curve. For non-singular curves the relation between order, n, and class, m, is $n = m(m-1)$. Hence, the order typically grows much more rapidly than the class. Order and class have the same value for $n = m = 2$.

3.4. *Circles, circular points at infinity*

So far the results obtained have had a pleasing duality between points and lines, but have not been particularly surprising. Consideration of a circle and its intersections with the ideal line provides unexpected answers.

Consider a circle in the affine plane

$$(x-a)^2 + (y-b)^2 = r^2. \tag{3.13}$$

Homogenize the expression as before to obtain

$$(x_1 - a x_3)^2 + (x_2 - b x_3)^2 = (r x_3)^2, \tag{3.14}$$

a 'circle' in $\boldsymbol{P}^2$. Now consider the intersection of this circle with the line at infinity, i.e. with points for which $x_3 = 0$. The equation for such points is

$$x_1^2 + x_2^2 = 0. \tag{3.15}$$

There are two solutions, (1, i, 0) and (1, $-$i, 0), regardless of the parameters a, b and r of the circle. These two points, usually designated I and J, respectively, are called the *circular points at infinity*. All circles pass through these two points.

A line is called *isotropic* if it passes through a circular point at infinity. Thus, except for the line at infinity, [0, 0, 1], which passes through both I and J, isotropic lines have coordinates of the form $[u_1, u_2, u_3] = [1, \pm \mathrm{i}, u_3]$.

3.5. *Foci*

An ellipse in the affine plane, situated and oriented appropriately, has the equation

$$\frac{x^2}{a^2} + \frac{y^2}{b^2} = 1, \tag{3.16}$$

with $a > b$. The two foci are at $(\pm c, 0)$, where $c = (a^2 - b^2)^{1/2}$. Homogenizing the equation for the ellipse we find

$$F(x_1, x_2, x_3) = \frac{x_1^2}{a^2} + \frac{x_2^2}{b^2} - x_3^2 = 0 \tag{3.17}$$

as the point equation in $\boldsymbol{P}^2$. Using the procedure outlined in §§3.2 and 3.3 we find the line equation to be

$$\Phi[u_1, u_2, u_3] = a^2 u_1^2 + b^2 u_2^2 - u_3^2 = 0. \tag{3.18}$$

As an illustration of this formalism we prove the result that *the product of the distances of the foci from a tangent is the same for all tangents* (and thus equal to the

square of the minor axis of the ellipse). Let $u_1 x + u_2 y + u_3 = 0$ be a tangent to the ellipse. The distances of the foci from this line are $(\pm u_1 c + u_3)/(u_1^2 + u_2^2)^{1/2}$, respectively. The product of distances is then $(u_3^2 - u_1^2 c^2)/(u_1^2 + u_2^2)$, which equals b^2 when $[u_1, u_2, u_3]$ satisfies (3.18). A similar argument holds for a hyperbola. It follows from replacing b by ib in the preceding.

We now inquire whether the ellipse has any isotropic tangents, i.e. whether $\Phi[1, \pm\mathrm{i}, u_3] = 0$ can be satisfied for any choice of u_3. Substitution into the equation gives $u_3 = \pm c$. Thus, there are four isotropic tangents:

$$[\boldsymbol{t}_1] = [1, \mathrm{i}, c]; \quad [\boldsymbol{t}_2] = [1, \mathrm{i}, -c]; \quad [\boldsymbol{t}_3] = [1, -\mathrm{i}, c]; \quad [\boldsymbol{t}_4] = [1, -\mathrm{i}, -c]. \tag{3.19}$$

These four lines intersect pairwise at four points (besides I and J):

$$(\boldsymbol{x}_{13}) = (-c, 0, 1); \quad (\boldsymbol{x}_{14}) = (0, \mathrm{i}c, 1); \quad (\boldsymbol{x}_{23}) = (0, -\mathrm{i}c, 1); \quad (\boldsymbol{x}_{24}) = (c, 0, 1). \tag{3.20}$$

We see that two of these points are in the affine plane, precisely at the focal points of the ellipse. This is a general result: *the focal points of a conic are the real intersections of the isotropic tangents.*

Let us write this out for the parabola. Start from $y = kx^2$. Homogenize: $kx_1^2 - x_2 x_3 = 0$. The line equation is: $u_1^2 - 4k u_2 u_3 = 0$. There are two isotropic tangents, $[1, \mathrm{i}, -\mathrm{i}/4k]$ and $[1, -\mathrm{i}, \mathrm{i}/4k]$; the line at infinity is also a tangent. There is, thus, just one finite point of intersection, $(0, 1/4k, 1)$, which, indeed, corresponds to the focus of the parabola in the affine plane.

In the general case, for a curve of class m, one defines the foci to be the intersections of the isotropic tangents. Except for degeneracies, there will be m^2 foci for such a curve. Of these m will be real and $m^2 - m$ complex.

In general, we must solve the equation $\Phi[1, \pm\mathrm{i}, u_3] = 0$ to find the isotropic tangents. Assuming Φ is real, i.e. a polynomial in u_1, u_2, u_3 with real coefficients, we see that if $u_3 = -z = -(x + \mathrm{i}y)$ is a solution of $\Phi[1, \mathrm{i}, -z] = 0$, then $z^* = x - \mathrm{i}y$ will solve

$$\Phi[1, -\mathrm{i}, -z^*] = 0.$$

The intersection of the two lines $[1, \mathrm{i}, -(x + \mathrm{i}y)]$ and $[1, -\mathrm{i}, -(x - \mathrm{i}y)]$ is easily calculated to be $(x, y, 1)$, a finite, real focus. All the real foci may be found in this way, and we have the result that *for a real curve of class m the foci in the affine plane, thought of as the complex z-plane, may be found from the equation*

$$\Phi[1, \mathrm{i}, -z] = 0. \tag{3.21}$$

It is this result, due to Plücker, that Siebeck exploits in his theorem, since the challenge is now simply to write the equation for the roots/stagnation points in such a way that it can be reinterpreted as determining the foci of a curve of the appropriate class.

3.6. *Siebeck's theorem*

Returning to (2.2) we wish, then, to write $P(z)$ in the form $\Phi[1, \mathrm{i}, -z]$. We set

$$L_\alpha[u_1, u_2, u_3] = -\xi_\alpha u_1 - \eta_\alpha u_2 - u_3, \tag{3.22}$$

where the αth vortex is at $z_\alpha = \xi_\alpha + \mathrm{i}\eta_\alpha$, $\alpha = 1, \ldots, N$, so that $L_\alpha[1, \mathrm{i}, -z] = z - z_\alpha$ (here we use Greek letters for the Cartesian coordinates of the vortices in order to avoid confusion with the coordinates x_1, x_2 and x_3 in $\boldsymbol{P}^2$). Consider

$$\begin{aligned}\Phi[u_1, u_2, u_3] = {} & \Gamma_1 L_2[u_1, u_2, u_3] L_3[u_1, u_2, u_3] \ldots L_N[u_1, u_2, u_3] \\ & + \Gamma_2 L_1[u_1, u_2, u_3] L_3[u_1, u_2, u_3] \ldots L_N[u_1, u_2, u_3] + \ldots \\ & + \Gamma_N L_1[u_1, u_2, u_3] L_2[u_1, u_2, u_3] \ldots L_{N-1}[u_1, u_2, u_3] = 0.\end{aligned} \tag{3.23}$$

This polynomial is constructed such that the term with pre-factor Γ_α contains the product of all $L_\beta[\boldsymbol{u}]$ except $\beta = \alpha$. Clearly this is a polynomial equation in the u of degree $N-1$, i.e. it defines a curve of class $N-1$. All coefficients are real (cf. (3.22)), so that the equation for the real, finite foci is

$$\Phi[1, \mathrm{i}, -z] = P(z) = 0. \tag{3.24}$$

Thus, the stagnation points may be interpreted as the real foci of the curve given by (3.23).

Furthermore, the curve has all the lines connecting the vortices pairwise as tangents, for the line through vortices α and β has coordinates (cf. (3.6))

$$[\boldsymbol{u}_{\alpha\beta}] = [\eta_\alpha - \eta_\beta, -(\xi_\alpha - \xi_\beta), \xi_\alpha \eta_\beta - \xi_\beta \eta_\alpha], \tag{3.25}$$

and both

$$L_\alpha[\boldsymbol{u}_{\alpha\beta}] = -\xi_\alpha(\eta_\alpha - \eta_\beta) + \eta_\alpha(\xi_\alpha - \xi_\beta) - (\xi_\alpha \eta_\beta - \xi_\beta \eta_\alpha) = 0, \tag{3.26a}$$

and

$$L_\beta[\boldsymbol{u}_{\alpha\beta}] = -\xi_\beta(\eta_\alpha - \eta_\beta) + \eta_\beta(\xi_\alpha - \xi_\beta) - (\xi_\alpha \eta_\beta - \xi_\beta \eta_\alpha) = 0. \tag{3.26b}$$

Since every term in Φ contains at least one of these as a factor, it follows that

$$\Phi[\boldsymbol{u}_{\alpha\beta}] = 0 \tag{3.27}$$

for all pairs (α, β). All the lines connecting vortices pairwise are thus tangent to (3.23).

The points of tangency may be found from the developments in §3.2. We are instructed to differentiate Φ with respect to u_1, u_2 and u_3, and substitute the line coordinates, $[\boldsymbol{u}_{\alpha\beta}]$, for the tangent in question. Calculating $\partial\Phi/\partial u_1$ we note that we only need to differentiate the terms containing Γ_α and Γ_β – all the other terms vanish when we substitute $[\boldsymbol{u}_{\alpha\beta}]$, since they will contain an undifferentiated factor L_α or L_β. We find

$$\frac{\partial \Phi}{\partial u_1}[\boldsymbol{u}_{\alpha\beta}] = -(\Gamma_\alpha \xi_\beta + \Gamma_\beta \xi_\alpha) \prod_{\gamma \neq \alpha, \beta} L_\gamma[\boldsymbol{u}_{\alpha\beta}], \tag{3.28a}$$

$$\frac{\partial \Phi}{\partial u_2}[\boldsymbol{u}_{\alpha\beta}] = -(\Gamma_\alpha \eta_\beta + \Gamma_\beta \eta_\alpha) \prod_{\gamma \neq a, b} L_\gamma[\boldsymbol{u}_{\alpha\beta}], \tag{3.28b}$$

$$\frac{\partial \Phi}{\partial u_3}[\boldsymbol{u}_{\alpha\beta}] = -(\Gamma_\alpha + \Gamma_\beta) \prod_{\gamma \neq \alpha, \beta} L_\gamma[\boldsymbol{u}_{\alpha\beta}]. \tag{3.28c}$$

Dividing by the common factor (the product of all L_γ with $\gamma \neq \alpha$, β evaluated for the line coordinates $[\boldsymbol{u}_{\alpha\beta}]$ – this quantity is non-zero unless three vortices are on a line), we see that the point of tangency is the point

$$z_{\alpha\beta}^{(S)} = \frac{\Gamma_\alpha z_\beta + \Gamma_\beta z_\alpha}{\Gamma_\alpha + \Gamma_\beta} \tag{3.29}$$

in the affine plane. This is the stagnation point for the flow produced by the two vortices α and β ignoring all the others.

This completes the proof of Siebeck's theorem, which in our context reads: *the stagnation points of the flow induced by N point vortices on the infinite plane are the foci of the curve* (3.23) *of class* $N-1$, *that touches each line connecting two vortices at the stagnation point of the flow produced by these two vortices ignoring all others.*

We now turn to particular cases.

4. The case of three vortices

Let us first note that the case of two vortices is trivial. Siebeck's curve has the equation

$$(\Gamma_1 \xi_2 + \Gamma_2 \xi_1) u_1 + (\Gamma_1 \eta_2 + \Gamma_2 \eta_1) u_2 + (\Gamma_1 + \Gamma_2) u_3 = 0 \tag{4.1}$$

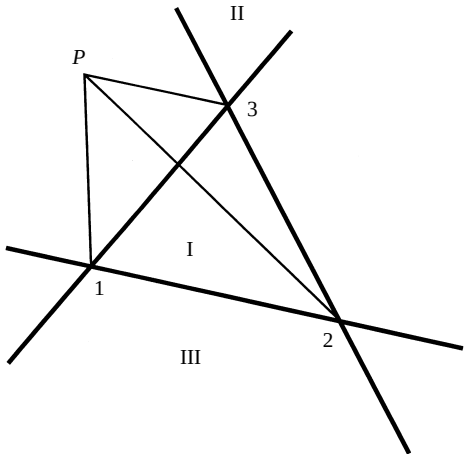

FIGURE 2. Illustration of the definition of triangular coordinates of an arbitrary point P relative to the vortex triangle 123. The regions I, II, and III, discussed in the text, are indicated.

in line coordinates. This is the equation for the point (1.7), the coordinates of which appear as the coefficients of u_1, u_2, u_3, i.e. (4.1) is the equation for all lines passing through this point (a curve in line coordinates of class 1 corresponds to a curve in point coordinates of order 0). Alternatively, the stagnation point is determined by setting $[u_1, u_2, u_3] = [1, \mathrm{i}, -z]$ in (4.1), which just gives the result (1.7).

4.1. *Triangular coordinates*

The case of three vortices is considerably richer. We know that the stagnation points are the foci of a conic, a curve of class 2, and we need to choose coordinates that facilitate the discussion of this curve. Assuming the vortices are not collinear, we may introduce new coordinates (X_1, X_2, X_3) in $\boldsymbol{P}^2$ via the equations

$$x_1 = \xi_1 X_1 + \xi_2 X_2 + \xi_3 X_3, \tag{4.2a}$$

$$x_2 = \eta_1 X_1 + \eta_2 X_2 + \eta_3 X_3, \tag{4.2b}$$

$$x_3 = X_1 + X_2 + X_3. \tag{4.2c}$$

Any finite point in $\boldsymbol{P}^2$, i.e. any point with $x_3 \neq 0$, will then have coordinates (X_1, X_2, X_3) with a sum that is different from zero. Since we are allowed to rescale, we choose to work with triples (X_1, X_2, X_3) that either have $X_1 + X_2 + X_3 = 1$, or that correspond to points on the line at infinity, i.e. have $X_1 + X_2 + X_3 = 0$. The benefit of this convention is that (X_1, X_2, X_3), when all three coordinates are real, may be interpreted as the *triangular coordinates* of a point in the plane based on the triangle spanned by the three vortices.† Thus, if a point P in the plane is connected to the vortices 1, 2 and 3, and the ratio of the areas of $\triangle 12P$, $\triangle 23P$, and $\triangle 31P$ to $\triangle 123$ itself, all calculated as signed quantities depending on orientation, are denoted X_1, X_2 and X_3, respectively, we always have $X_1 + X_2 + X_3 = 1$. The construction is illustrated in figure 2 for a case in which $\triangle 12P$, $\triangle 23P$ and $\triangle 123$ (and thus X_1 ad X_3) are all positive, whereas $\triangle 31P$ (and thus X_2) is negative.

† The treatise by Ferrers (1866) is concerned with trilinear and triangular coordinates and their geometrical applications; for an informal discussion of applications of such coordinates in fluid mechanics see Aref (1992).

A point (ξ, η) in the affine plane corresponds to $(\xi, \eta, 1)$ in $\boldsymbol{P}^2$, and has triangular coordinates

$$X_1 = \frac{\xi\eta_2 - \xi_2\eta + \xi_2\eta_3 - \xi_3\eta_2 + \xi_3\eta - \xi\eta_3}{\xi_1\eta_2 - \xi_2\eta_1 + \xi_2\eta_3 - \xi_3\eta_2 + \xi_3\eta_1 - \xi_1\eta_3}, \tag{4.3a}$$

$$X_2 = \frac{\xi_1\eta - \xi\eta_1 + \xi\eta_3 - \xi_3\eta + \xi_3\eta_1 - \xi_1\eta_3}{\xi_1\eta_2 - \xi_2\eta_1 + \xi_2\eta_3 - \xi_3\eta_2 + \xi_3\eta_1 - \xi_1\eta_3}, \tag{4.3b}$$

$$X_3 = \frac{\xi_1\eta_2 - \xi_2\eta_1 + \xi_2\eta - \xi\eta_2 + \xi\eta_1 - \xi_1\eta}{\xi_1\eta_2 - \xi_2\eta_1 + \xi_2\eta_3 - \xi_3\eta_2 + \xi_2\eta_1 - \xi_1\eta_3}. \tag{4.3c}$$

The denominator in these expressions is twice the signed area of $\triangle 123$.

There is a corresponding transformation of line coordinates:

$$U_1 = \xi_1 u_1 + \eta_1 u_2 + u_3, \tag{4.4a}$$

$$U_2 = \xi_2 u_1 + \eta_2 u_2 + u_3, \tag{4.4b}$$

$$U_3 = \xi_3 u_1 + \eta_3 u_2 + u_3, \tag{4.4c}$$

to ensure that $u_1 x_1 + u_2 x_2 + u_3 x_3 = U_1 X_1 + U_2 X_2 + U_3 X_3$.

The inverse transformation is

$$u_1 = \frac{U_1\eta_2 - U_2\eta_1 + U_2\eta_3 - U_3\eta_2 + U_3\eta_1 - U_1\eta_3}{\xi_1\eta_2 - \xi_2\eta_1 + \xi_2\eta_3 - \xi_3\eta_2 + \xi_3\eta_1 - \xi_1\eta_3}, \tag{4.5a}$$

$$u_2 = \frac{\xi_1 U_2 - \xi_2 U_1 + \xi_2 U_3 - \xi_3 U_2 + \xi_3 U_1 - \xi_1 U_3}{\xi_1\eta_2 - \xi_2\eta_1 + \xi_2\eta_3 - \xi_3\eta_2 + \xi_3\eta_1 - \xi_1\eta_3}, \tag{4.5b}$$

$$u_3 = \frac{(\xi_1\eta_2 - \xi_2\eta_1)\,U_3 + (\xi_2\eta_3 - \xi_3\eta_2)\,U_1 + (\xi_3\eta_1 - \xi_1\eta_3)\,U_2}{\xi_1\eta_2 - \xi_2\eta_1 + \xi_2\eta_3 - \xi_3\eta_2 + \xi_3\eta_1 - \xi_1\eta_3}. \tag{4.5c}$$

The line at infinity, $[\boldsymbol{u}] = [0, 0, 1]$, has coordinates $[\boldsymbol{U}] = [1, 1, 1]$, and thus corresponds to the 'unphysical' condition $X_1 + X_2 + X_3 = 0$.

The triangular coordinates of the vortices are, of course, $(\boldsymbol{X}) = (1, 0, 0)$ for vortex 1; (0, 1, 0) for 2; (0, 0, 1) for 3. The line coordinates of the sides are $[\boldsymbol{U}] = [0, 0, 1]$ for the side 12; [1, 0, 0] for 23; [0, 1, 0] for 31. In these coordinates the expression for Φ simplifies considerably, as is seen by comparing (4.4) to (3.22). The line conic (3.23) becomes

$$\Gamma_1 U_2 U_3 + \Gamma_2 U_1 U_3 + \Gamma_3 U_1 U_2 = 0. \tag{4.6}$$

Differentiating we find the point conic as follows:†

$$X_1 = \Gamma_2 U_3 + \Gamma_3 U_2, \quad X_2 = \Gamma_3 U_1 + \Gamma_1 U_3, \quad X_3 = \Gamma_1 U_2 + \Gamma_2 U_1. \tag{4.7}$$

Solving these for the U in terms of the X gives

$$2\Gamma_2\Gamma_3 U_1 = -\Gamma_1 X_1 + \Gamma_2 X_2 + \Gamma_3 X_3, \tag{4.8a}$$

$$2\Gamma_3\Gamma_1 U_2 = \Gamma_1 X_1 - \Gamma_2 X_2 + \Gamma_3 X_3, \tag{4.8b}$$

$$2\Gamma_1\Gamma_2 U_3 = \Gamma_1 X_1 + \Gamma_2 X_2 - \Gamma_3 X_3. \tag{4.8c}$$

† It is not difficult to see that the procedure given in §3.2 for transforming between line and point coordinates of a curve carries over to the new variables $\boldsymbol{X}$ and $\boldsymbol{U}$. Statements involving actual values of coordinates, however, need to be carefully reinterpreted. For example, the coordinates of the circular points at infinity, §3.4, are more complicated in terms of the variables $\boldsymbol{X}$ than in terms of the original variables $\boldsymbol{x}$.

Substituting these expressions in the equation for the line conic gives the equation for the point conic in triangular coordinates:

$$(\Gamma_1 X_1)^2+(\Gamma_2 X_2)^2+(\Gamma_3 X_3)^2 = 2\Gamma_1\Gamma_2 X_1 X_2+2\Gamma_2\Gamma_3 X_2 X_3+2\Gamma_3\Gamma_1 X_3 X_1. \quad (4.9)$$

The points of tangency with the triangle spanned by the vortices are

$$(\boldsymbol{X}_{23}) = \left(0, \frac{\Gamma_3}{\Gamma_2+\Gamma_3}, \frac{\Gamma_2}{\Gamma_2+\Gamma_3}\right), \quad (4.10a)$$

$$(\boldsymbol{X}_{31}) = \left(\frac{\Gamma_3}{\Gamma_3+\Gamma_1}, 0, \frac{\Gamma_1}{\Gamma_3+\Gamma_1}\right), \quad (4.10b)$$

$$(\boldsymbol{X}_{12}) = \left(\frac{\Gamma_2}{\Gamma_1+\Gamma_2}, \frac{\Gamma_1}{\Gamma_1+\Gamma_2}, 0\right). \quad (4.10c)$$

We see that the three lines

$$\Gamma_1 X_1 = \Gamma_2 X_2 = \Gamma_3 X_3, \quad (4.11a)$$

or, in line coordinates,

$$[\boldsymbol{U}] = [\Gamma_1, -\Gamma_2, 0]; \quad [-\Gamma_1, 0, \Gamma_3]; \quad [0, \Gamma_2, -\Gamma_3]; \quad (4.11b)$$

connect a vortex to the point of tangency on the opposing side (4.10). The lines (4.11) are concurrent at a point T with coordinates

$$(X_1^{(T)}, X_2^{(T)}, X_3^{(T)}) = (\Gamma_2\Gamma_3, \Gamma_3\Gamma_1, \Gamma_1\Gamma_2)/(\Gamma_1\Gamma_2+\Gamma_2\Gamma_3+\Gamma_3\Gamma_1) \quad (4.12)$$

(which is at infinity if the harmonic mean of the vortex strengths vanishes).

The conic (4.9) is, except for a change in notation, the same as was considered in an earlier analysis of three-vortex motion (see Aref 1979, equation (14)). It follows, therefore, that the classification of the nature of the conic that has the stagnation points as foci in terms of the values of the vortex strengths is exactly the classification of the motion itself found in the earlier work.† In particular, the stagnation point conic is

$$\text{an ellipse if} \quad \Gamma_1\Gamma_2\Gamma_3(\Gamma_1+\Gamma_2+\Gamma_3) > 0, \quad (4.13a)$$

$$\text{a parabola if} \quad \Gamma_1+\Gamma_2+\Gamma_3 = 0, \quad (4.13b)$$

$$\text{a hyperbola if} \quad \Gamma_1\Gamma_2\Gamma_3(\Gamma_1+\Gamma_2+\Gamma_3) < 0. \quad (4.13c)$$

The type of this conic depends only on the vortex strengths, and thus is invariant in time (except for the degeneracy that occurs when the vortices are on a line and the conic collapse to a line segment). Indeed, the equation of the inscribed conic in triangular coordinates, (4.9), is invariant with respect to the shape of the vortex triangle, and thus *a fortiori* the classification, (4.13), of whether it is an ellipse, a parabola or a hyperbola will be invariant with respect to the evolution of that triangle in time as the motion unfolds.

Our results thus far establish several qualitative differences between the (two) elliptic, parabolic and hyperbolic cases regarding the location of stagnation points. The lines connecting the vortices pairwise divide the plane into seven regions. Without loss of generality we restrict consideration to the case $\Gamma_1 \geqslant \Gamma_2 > 0$, since other choices of signs follow by re-labelling of indices and/or reflection in the flow plane. Then, in figure 2, the stagnation points in the elliptic cases will either both be in region I (for

† The formal way to decide this is to write out the coefficient matrix of the quadratic (4.9), convert back to variables x_1, x_2, x_3 via (4.2) and consider the determinant of the appropriate minor (cf. the text following (3.9)).

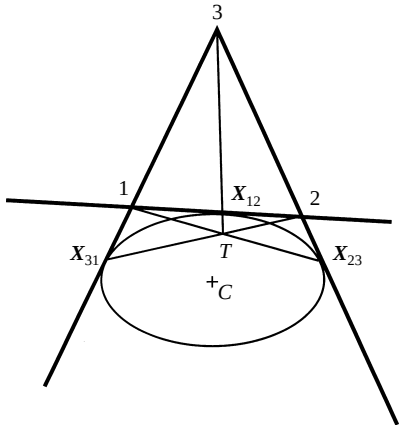

FIGURE 3. Relative situation of vortices (1, 2 and 3), Siebeck's conic with centre C, the three points of tangency, $\boldsymbol{X}_{12}$, $\boldsymbol{X}_{23}$, $\boldsymbol{X}_{31}$ and the point of concurrency, T, of $1\boldsymbol{X}_{23}$, $2\boldsymbol{X}_{31}$, and $3\boldsymbol{X}_{12}$. The lines $1C$, $2C$ and $3C$ bisect $\boldsymbol{X}_{31}\,\boldsymbol{X}_{12}$, $\boldsymbol{X}_{12}\,\boldsymbol{X}_{23}$ and $\boldsymbol{X}_{23}\,\boldsymbol{X}_{31}$, respectively.

$\Gamma_3 > 0$), or in region III (for $\Gamma_3 < 0$) since the ellipse will be situated in one of these two regions (see figure 3 for an example when $\Gamma_3 < 0$). In the hyperbolic case there will be one stagnation point in region II and one in region III since the hyperbola will have a branch in each of these two regions. Thus, in this case, so long as the vortices are not collinear, there must always be two distinct stagnation points, whereas in the elliptic case the two stagnation points can coincide when the ellipse degenerates to a circle. In the parabolic case, the single stagnation point will always be in region III since this is where the parabola will be located. This immediate consequence of the geometric characterization of stagnation points is not obvious if one simply proceeds to find the roots of the polynomial (2.2) algebraically. For the case of positive vortex strengths the Gauss–Lucas theorem (cf. Marden 1949, Chap. II) implies that the stagnation points must lie within the triangle spanned by the vortices. The location as foci of an inscribed ellipse is clearly much sharper.

4.2. *Elliptic and hyperbolic cases*

In the elliptic and hyperbolic case let the triangular coordinates of the two stagnation points be (X_1, X_2, X_3) and $(\tilde{X}_1, \tilde{X}_2, \tilde{X}_3)$, respectively. From (2.8) we deduce that

$$X_1+\tilde{X}_1 = \frac{\Gamma_2+\Gamma_3}{\Gamma_1+\Gamma_2+\Gamma_3}, \quad X_2+\tilde{X}_2 = \frac{\Gamma_3+\Gamma_1}{\Gamma_1+\Gamma_2+\Gamma_3}, \quad X_3+\tilde{X}_3 = \frac{\Gamma_1+\Gamma_2}{\Gamma_1+\Gamma_2+\Gamma_3}. \quad (4.14)$$

The centre of the conic in Siebeck's theorem, C, must then have triangular coordinates

$$(X_1^{(C)}, X_2^{(C)}, X_3^{(C)}) = \left(\frac{\Gamma_2+\Gamma_3}{2(\Gamma_1+\Gamma_2+\Gamma_3)}, \frac{\Gamma_3+\Gamma_1}{2(\Gamma_1+\Gamma_2+\Gamma_3)}, \frac{\Gamma_1+\Gamma_2}{2(\Gamma_1+\Gamma_2+\Gamma_3)}\right). \quad (4.15)$$

These coordinates are also invariant with respect to the actual configuration of the vortices (i.e. the shape of the triangle) and – since they depend only on the vortex strengths – with respect to the motion.

It is easy to verify that the line connecting vortex 1 to C bisects the line connecting the points of tangency $(\boldsymbol{X}_{31})$ and $(\boldsymbol{X}_{12})$, with corresponding results by permutation of indices. Figure 3 summarizes the relative situation and role of the points of tangency

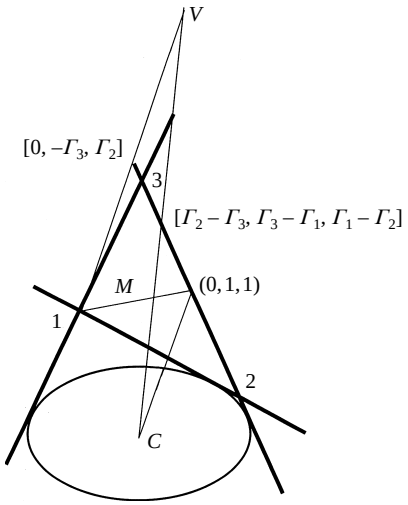

FIGURE 4. Geometry of the midpoint, M, centre of vorticity, V, and centre of Siebeck's conic, C. Note that M, V and C are collinear and $CM:MV = 1:2$.

and the points T and C. It is important not to confuse the points T (point of concurrency of lines connecting vortices to points of tangency) and C (centre of Siebeck's conic).

Since the centre of Siebeck's conic is situated at the midpoint of the line joining the two stagnation points, we note from (2.9) that this point must be on the line through the centroid of the vortex configuration and the centre of vorticity. Alternatively, we may verify directly that the line $[\boldsymbol{U}] = [\Gamma_2-\Gamma_3,\ \Gamma_3-\Gamma_1,\ \Gamma_1-\Gamma_2]$ passes through the centroid, $(\boldsymbol{X}) = (1,\ 1,\ 1)$, the centre of vorticity, $(\Gamma_1,\ \Gamma_2,\ \Gamma_3)/(\Gamma_1+\Gamma_2+\Gamma_3)$, and the point C given by (4.15). Designating the complex position of C by z_C, and recalling our earlier definitions of z_M and z_V from §2, we have

$$z_C = \tfrac{3}{2} z_M - \tfrac{1}{2} z_V. \tag{4.16}$$

This relation shows, further, that the midpoint splits the line segment connecting the centre of the conic to the centre of vorticity in the ratio 1:2. Since the midpoint itself splits each median in the vortex triangle in this ratio, the following construction of the point C presents itself (figure 4). From the instantaneous vortex positions and the vortex strengths determine the centre of vorticity. Draw the line $[\Gamma_2-\Gamma_3,\ \Gamma_3-\Gamma_1,\ \Gamma_1-\Gamma_2]$ through the midpoint of the triangle and the centre of vorticity (we list the coordinates so that the construction can be verified algebraically). Join any vortex, e.g. 1 as shown in figure 4, to the centre of vorticity, producing a line with coordinates $[0,\ -\Gamma_3,\ \Gamma_2]$. Through the midpoint (0, 1, 1) of the opposite side in the vortex triangle draw the line parallel to $[0,\ -\Gamma_3,\ \Gamma_2]$. This is the line $[\Gamma_2-\Gamma_3,\ \Gamma_2+\Gamma_3,\ -(\Gamma_2+\Gamma_3)]$ – 'parallelism' in triangular coordinates means that two lines intersect on the line [1, 1, 1]. Point C, the centre of Siebeck's conic, is then found at the intersection of $[\Gamma_2-\Gamma_3,\ \Gamma_3-\Gamma_1,\ \Gamma_1-\Gamma_2]$ and $[\Gamma_2-\Gamma_3,\ \Gamma_2+\Gamma_3,\ -(\Gamma_2+\Gamma_3)]$, as is easily verified.

From the result on the product of the distances of the foci from a tangent (see §3.5 following (3.18)) we have

$$\frac{X_1\tilde{X}_1}{d_{23}^2} = \frac{X_2\tilde{X}_2}{d_{31}^2} = \frac{X_3\tilde{X}_3}{d_{12}^2}, \tag{4.17}$$

where d_{12}, d_{23} and d_{31} are the lengths of the sides of the triangle (using an obvious

notation). The common value of the expressions in (4.17) is positive in the elliptic case and negative in the hyperbolic case.

Combining (4.14) and (4.17) the triangular coordinates of the stagnation points of three vortices must solve the system of equations

$$\begin{aligned}\frac{1}{d_{23}^2}\{(\Gamma_1+\Gamma_2+\Gamma_3)\,X_1-(\Gamma_2+\Gamma_3)\}\,X_1 \\ =\frac{1}{d_{31}^2}\{(\Gamma_1+\Gamma_2+\Gamma_3)\,X_2-(\Gamma_3+\Gamma_1)\}\,X_2 \\ =\frac{1}{d_{12}^2}\{(\Gamma_1+\Gamma_2+\Gamma_3)\,X_3-(\Gamma_1+\Gamma_2)\}\,X_3,\end{aligned} \tag{4.18a}$$

with

$$X_1+X_2+X_3=1. \tag{4.18b}$$

Ferrers (1866, Chap. VI, §33) finds equations equivalent to (4.18) using the theory of reciprocal polars.

In order to solve (4.18) we set the common value of the three expressions to $k(\Gamma_1+\Gamma_2+\Gamma_3)$. Then we find

$$X_1=X_1^{(C)}\pm((X_1^{(C)})^2+kd_{23}^2)^{1/2}, \tag{4.19a}$$

$$X_2=X_2^{(C)}\pm((X_2^{(C)})^2+kd_{31}^2)^{1/2}, \tag{4.19b}$$

$$X_3=X_3^{(C)}\pm((X_3^{(C)})^2+kd_{12}^2)^{1/2}. \tag{4.19c}$$

It follows from these that

$$\pm((X_1^{(C)})^2+kd_{23}^2)^{1/2}\pm((X_2^{(C)})^2+kd_{31}^2)^{1/2}\pm((X_3^{(C)})^2+kd_{12}^2)^{1/2}=0. \tag{4.20}$$

Squaring twice (4.20) yields a quadratic equation for k:

$$\begin{aligned}&k^2(d_{12}^4+d_{23}^4+d_{31}^4-2d_{12}^2d_{23}^2-2d_{23}^2d_{31}^2-2d_{31}^2d_{12}^2)\\&+2k[d_{12}^2\{(X_3^{(C)})^2-(X_1^{(C)})^2-(X_2^{(C)})^2\}+d_{23}^2\{(X_1^{(C)})^2-(X_2^{(C)})^2-(X_3^{(C)})^2\}\\&\quad+d_{31}^2\{(X_2^{(C)})^2-(X_3^{(C)})^2-(X_1^{(C)})^2\}]\\&+(X_1^{(C)})^4+(X_2^{(C)})^4+(X_3^{(C)})^4-2(X_1^{(C)})^2(X_2^{(C)})^2-2(X_2^{(C)})^2(X_3^{(C)})^2-2(X_3^{(C)})^2(X_1^{(C)})^2=0.\end{aligned} \tag{4.21}$$

The coefficient of k^2 in (4.21) is $(4\Delta)^2$ by Hero's formula for the area of a triangle. The constant term can be simplified to $-\Gamma_1\Gamma_2\Gamma_3/(\Gamma_1+\Gamma_2+\Gamma_3)^3$. The coefficient of k is

$$\{d_{12}^2(\Gamma_1\Gamma_2-\Gamma_3\Sigma)+d_{23}^2(\Gamma_2\Gamma_3-\Gamma_1\Sigma)+d_{31}^2(\Gamma_3\Gamma_1-\Gamma_2\Sigma)\}/\Sigma^2, \tag{4.22}$$

where the abbreviation $\Sigma=\Gamma_1+\Gamma_2+\Gamma_3$ has been used.

Equation (4.21) will, in general, have two real solutions for k. For each of these (4.19) with the two sign choices provides as many as eight solutions. From these 16 triples (X_1, X_2, X_3) only two are acceptable as solutions for the stagnation points. We shall not pause here to sort out the signs in (4.19). We do make the point, however, that the triangular coordinates of the stagnation points will not for a generic choice of Γ_1, Γ_2 and Γ_3 conform to any simple scaling or similarity relation. Surprisingly, such scaling does arise in the parabolic case discussed below.

The hyperbolic case $\Gamma_1 = \Gamma_2 = -\Gamma_3 = \Gamma$ is so simple that a complete discussion may be given. We see from (4.10) that two of the points of tangency are at infinity, i.e. the lines 23 and 31 are the asymptotes of the hyperbola (4.9). The centre of this conic, then, is vortex 3, as given by (4.15). Equations (4.18) simplify to

$$\frac{X_1^2}{d_{23}^2} = \frac{X_2^2}{d_{31}^2} = \frac{X_3^2 - 2X_3}{d_{12}^2}. \tag{4.23}$$

The first equality shows that the stagnation points are located on the bisector of $\angle 231$. With this information one can either return to the original equation (2.1) or rework the second equality in (4.19) to show that the distance from vortex 3 to either stagnation point is $(d_{23}\, d_{31})^{1/2}$, the geometric mean of the two sides of the triangle that are along the asymptotes of Siebeck's conic.

4.3. *The parabolic case*

In the parabolic case the first term in the curly brackets in (4.18*a*), vanishes, and for the single stagnation point we now have†

$$\Gamma_1 X_1 = k d_{23}^2; \quad \Gamma_2 X_2 = k d_{31}^2; \quad \Gamma_3 X_3 = k d_{12}^2. \tag{4.24}$$

In (4.24) k is the common value of the expressions (4.18*a*), and we have used that the vortex strengths sum to zero. Multiplying by $\Gamma_2\,\Gamma_3$, $\Gamma_3\,\Gamma_1$, $\Gamma_1\,\Gamma_2$, respectively, adding and using (4.18*b*) we obtain

$$k = \frac{\Gamma_1 \Gamma_2 \Gamma_3}{\Gamma_1 \Gamma_2 d_{12}^2 + \Gamma_2 \Gamma_3 d_{23}^2 + \Gamma_3 \Gamma_1 d_{31}^2}. \tag{4.25}$$

Thus the triangular coordinates of the stagnation point in the parabolic case are

$$(X_1^{(S)}, X_2^{(S)}, X_3^{(S)}) = \frac{(\Gamma_2 \Gamma_3 d_{23}^2, \Gamma_3 \Gamma_1 d_{31}^2, \Gamma_1 \Gamma_2 d_{12}^2)}{\Gamma_1 \Gamma_2 d_{12}^2 + \Gamma_2 \Gamma_3 d_{23}^2 + \Gamma_3 \Gamma_1 d_{31}^2}. \tag{4.26}$$

The denominator is a constant of the motion (cf. Aref 1979). Hence, we have the 'similarity' result that *in the parabolic case the triangular coordinates of the stagnation point, each scaled by the square of the corresponding side in the vortex triangle, are constant during the motion*. This result is quite remarkable, since the stagnation point is not invariant in an Eulerian or Lagrangian sense, and does not, in general, have a fixed position relative to the vortices.

When the denominator in (4.26) vanishes, there is no finite stagnation point. This may be seen either by referring to the explicit solution available for this case (Rott 1989; Aref 1989),‡ or simply by noting that the linear impulse must also vanish, and we are in the situation discussed following (2.6) in which $P(z)$ reduces to a constant for $N = 3$.

Another way to state the result (4.26) arises from the expressions $X_1^{(S)} = h_1^{(S)}\, d_{23}/2\Delta$,

† One might worry that (4.24) arises from (4.18) by using (4.14), and this condition is ambiguous when one focus is at infinity. However, an independent derivation shows that (4.24) are, indeed, the correct equations for the focus in the parabolic case.

‡ This solution may be written $z_1 = a(\Gamma_3/\Gamma_2 - \Gamma_2/\Gamma_3)$, $z_2 = a(\Gamma_1/\Gamma_3 - \Gamma_3/\Gamma_1)$, $z_3 = a(\Gamma_2/\Gamma_1 - \Gamma_1/\Gamma_2)$, where a is a scale parameter, i.e. the vortices are situated on a line, and rotate with angular velocity $\Gamma_1\,\Gamma_2\,\Gamma_3/2\pi a(\Gamma_1\,\Gamma_2 + \Gamma_2\,\Gamma_3 + \Gamma_3\,\Gamma_1)$ about the origin of coordinates, but the velocity at the origin does not vanish. If $\Gamma_1 = \Gamma_2$ and vortices 1 and 2 are placed on either side of vortex 3 at equal distances from it, the configuration will rotate about vortex 3, which will remain stationary. This kind of stagnation point is not covered by the developments in this paper.

etc., where $h_1^{(S)}$ denotes the distance of the stagnation point from the side 23. Substituting this form for the triangular coordinates into (4.26), we obtain

$$\left(\frac{h_1^{(S)}}{d_{23}}, \frac{h_2^{(S)}}{d_{31}}, \frac{h_3^{(S)}}{d_{12}}\right) = \frac{2\Delta(\Gamma_2\Gamma_3, \Gamma_3\Gamma_1, \Gamma_1\Gamma_2)}{\Gamma_1\Gamma_2 d_{12}^2 + \Gamma_2\Gamma_3 d_{23}^2 + \Gamma_3\Gamma_1 d_{31}^2}. \tag{4.27}$$

Hence, the dimensionless ratio of the distance of the stagnation point from a side to the length of that side varies proportionally to the vortex triangle area.

It is not difficult to show (cf. Ferrers 1866, Art. 6) that the equation for the circumscribed circle of the vortex triangle is

$$d_{12}^2 X_1 X_2 + d_{23}^2 X_2 X_3 + d_{31}^2 X_3 X_1 = 0. \tag{4.28}$$

We see that the stagnation point (4.26) is situated on this circle.

5. Streamline topology

We now turn to the second mode of analysis of the flow pattern surrounding a set of discrete vortices – a topological exploration of possible streamline patterns. The vortices themselves must be encircled by a system of nested streamlines. The stagnation points, on the other hand, are points of self-intersection of streamlines. Since we have seen how to geometrically characterize the stagnation points given the location and strength of the vortices, it is natural to explore how to connect these stagnation points by streamlines to determine the overall, instantaneous flow pattern. As we shall see, for a small number of vortices this leads to a relatively small set of topologically distinct possibilities. We shall discuss the cases $N = 2$ and 3 in detail, but the methodology used can, in principle, be extended to larger N.

For the case of two point vortices it is not difficult to see that the flow topology must be invariant as the motion proceeds: the location of the vortices and the stagnation point simply rotate rigidly about the centre of vorticity, and so the entire streamline configuration must also rotate about this point.

For two vortices there are three distinct streamline topologies with a single stagnation point, as indicated in figure 5. There is just one pattern for two opposite vortices, figure 5(*d*).

5.1. *Streamline topologies for three vortices*

For three vortices the situation is richer. Let us first consider the elliptic and hyperbolic cases for which there are two stagnation points. Since the sum of the vortex strengths is different from zero, the far-field velocity at any instant is like the flow due to a single vortex of strength equal to this sum. In particular, no streamlines go off to infinity. It then follows that the streamlines must form a pattern in which the two stagnation points are connected, either to themselves or to each other, and a simple enumeration of the topological possibilities accounts for the different types of flow.

Borrowing from the dynamical systems nomenclature we designate a streamline loop connecting a stagnation point to itself as a *homoclinic loop*, and we designate two streamline segments connecting two stagnation points as a *heteroclinic loop*. Heteroclinic loops occur only if the streamfunction of the flow takes the same value at both stagnation points. This will not generally be the case, and so signifies a special vortex configuration at which a bifurcation of the streamline pattern takes place. The typical streamline topology will consist solely of homoclinic loops.

In order to find these, we return to figure 5 and consider the pattern 5(*a*) or 5(*b*) to be 'substituted' for either positive vortex in 5(*a*). This gives the streamline topologies

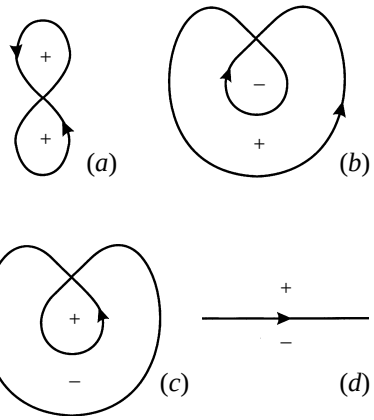

FIGURE 5. Streamline topologies for flow about two vortices. For non-zero net circulation there is one stagnation point: (*a*) two positive vortices; (*b*) a vortex of either sign with the sum of strengths positive; (*c*) a vortex of either sign with the sum of strengths negative. In (*d*) the vortices are opposite.

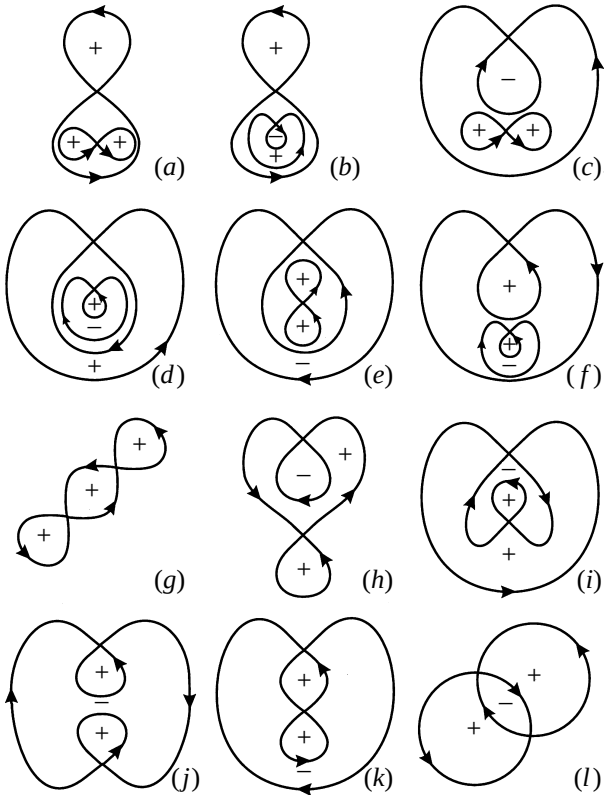

FIGURE 6. Streamline topologies for flow about three vortices with non-zero net circulation, $\Gamma_1+\Gamma_2+\Gamma_3 \neq 0$. The derivation of the different cases is discussed in the text. Patterns (*a*)–(*f*) have no heteroclinic loops and are the 'generic' cases. Patterns (*g*)–(*k*) have one heteroclinic loop, (*l*) has three. Streamline topologies (*a*, *e*, *f*, *g*, *j*, *k*) are for the elliptic cases; (*b*, *c*, *d*, *h*, *i*, *l*) for the hyperbolic.

in figure 6(*a*, *b*). In generating from figure 5(*b*) a possible streamline topology for three vortices our sign convention dictates that the pattern 5(*a*) can be substituted for the positive vortex, leading to figure 6(*c*), but not the pattern 5(*b*), since that would produce a pattern with two negative vortices. However, the pattern 5(*c*) can be

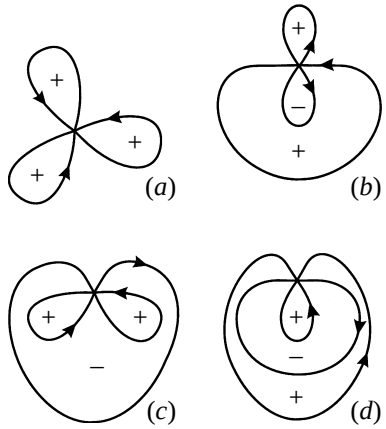

FIGURE 7. Streamline topologies for flow about three vortices with non-zero net circulation, $\Gamma_1+\Gamma_2+\Gamma_3 \neq 0$ in the degenerate cases with a single stagnation point; (*a*), (*c*) are elliptic cases, (*b*), (*d*) hyperbolic.

substituted for the negative vortex in 5(*b*) leading to figure 6(*d*). Again, in figure 5(*c*) we may substitute 5(*a*) for the positive vortex, producing figure 6(*e*), or 5(*c*) for the negative vortex, producing figure 6(*f*). All these patterns have four homoclinic loops, and exhaust the possibilities for patterns with all homoclinic loops.

If we start from figure 5(*a*) and somewhere along either homoclinic loop 'pinch off' a new homoclinic loop, we produce the streamline topologies in figures 6(*g*) and 6(*h*) depending on whether the 'pinched off' loop is outside or inside one of the existing homoclinic loops. A similar transformation applied to figure 5(*b*) – where we are only allowed to place a loop outside the positive vortex loop or inside the negative vortex loop, since we otherwise would produce a second negative vortex – yields figure 6(*i*) (and a repeat of 6*h*). From figure 5(*c*) we similarly produce figures 6(*j*) and 6(*k*). All these streamline patterns have two homoclinic loops and one heteroclinic loop. Conversely, by letting a homoclinic loop in figure 6(*g–k*) shrink to a point (if allowed by the presence of the remaining two vortices) we reproduce one of the streamline topologies from figure 5. Finally, figure 6(*l*) shows the single possibility when there are no homoclinic loops. These 12 streamline patterns are the only ones possible for three vortices on the infinite plane when the sum of strengths is non-zero. By considering the sense of the far-field flow in these diagrams we see that figure 6(*a*, *e*, *f*, *g*, *j*, *k*) corresponds to elliptic cases, whereas figure 6(*b*, *c*, *d*, *h*, *i*, *l*) corresponds to hyperbolic cases.

There are four degenerate cases in which there is only a single stagnation point, where three streamline branches divide the plane into six sectors each of opening angle $\pi/3$. They can be determined by drawing the three streamline segments close to the degenerate stagnation point, and then connecting these segments to form loops in all possible ways (consistent with our sign convention on vortex strengths). The resulting four patterns are shown in figure 7.

There is a simple algebraic condition, which follows from (4.14) and (4.17), for when such degeneracy occurs. In the elliptic case the stagnation points can coincide because Siebeck's conic – which is an ellipse in this case – can degenerate to a circle. Thus, setting $(X_1, X_2, X_3) = (\tilde{X}_1, \tilde{X}_2, \tilde{X}_3) = (X_1^{(C)}, X_2^{(C)}, X_3^{(C)})$, we find the condition

$$\left(\frac{\Gamma_2+\Gamma_3}{d_{23}}\right)^2 = \left(\frac{\Gamma_3+\Gamma_1}{d_{31}}\right)^2 = \left(\frac{\Gamma_1+\Gamma_2}{d_{12}}\right)^2, \tag{5.1}$$

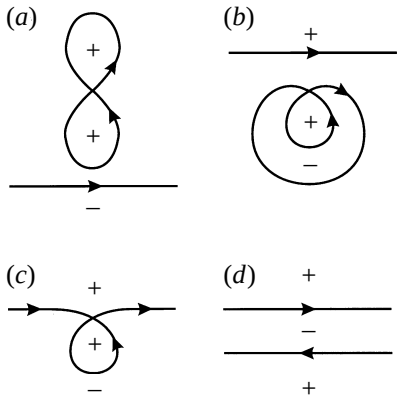

FIGURE 8. Streamline topologies for flow about three vortices with zero net circulation, $\Gamma_1+\Gamma_2+\Gamma_3=0$.

which determines the shape of the vortex triangle. Since $\Gamma_1+\Gamma_3$ and $\Gamma_2+\Gamma_3$ are of the same sign in this case, (5.1) may be written

$$\frac{\Gamma_2+\Gamma_3}{d_{23}}=\frac{\Gamma_3+\Gamma_1}{d_{31}}=\pm\frac{\Gamma_1+\Gamma_2}{d_{12}}, \tag{5.2}$$

where the sign in the last term is the sign of Γ_3. Thus, if the vortices form an equilateral triangle, the two stagnation points will coincide if $\Gamma_1=\Gamma_2=\Gamma_3$, but also if $\Gamma_1:\Gamma_2:\Gamma_3=1:1:(-3)$. In the former case we get the streamline pattern figure 7(*a*), in the latter figure 7(*c*).

In the hyperbolic case the two stagnation points (alias foci of a hyperbola) can only coincide if the vortices are collinear. Hence, the patterns in figures 7(*b*) and 7(*d*) must arise from collinear vortices. In particular, in the collinear state the negative vortex must always be situated between the positive vortices in order for a degenerate stagnation point to arise.

The streamline patterns for the parabolic case are constructed by a similar method of 'substitution' starting from the pattern in figure 5(*d*) for two vortices of net circulation zero. We can substitute the pattern 5(*a*) for the positive vortex in 5(*d*) resulting in figure 8(*a*). We can substitute 5(*c*) for the negative vortex in 5(*d*) producing figure 8(*b*). We can 'pinch off' a homoclinic loop on the single dividing streamline in 5(*d*) to produce a positive vortex resulting in figure 8(*c*). These are the only non-degenerate forms. However, the stagnation point at infinity in figure 5(*d*) could be degenerate, and this results in the pattern in figure 8(*d*). Alternatively, the patterns in figure 8(*a–d*) can be thought of as limiting forms of the elliptic patterns in figure 6(*e*, *f*, *k*, *j*), respectively.

It must be kept in mind that the diagrams of figures 5–8 give the possible streamline topologies without regard to scale. When actual values are substituted for the vortex strengths, and the diagrams are accurately constructed, the relative size of the various loops may be quite different from what is shown in figures 5–8. We have plotted in figure 9 some such correctly scaled streamline patterns for certain chosen vortex positions and strengths. Two additional examples of streamline patterns 'to scale' have already been given in figure 1.

The construction of the different streamline topologies given above assures us that all the topologies identified in figures 5–8 will actually occur for suitable choices of vortex positions and strengths, and shows, in principle, how to generate them. One can

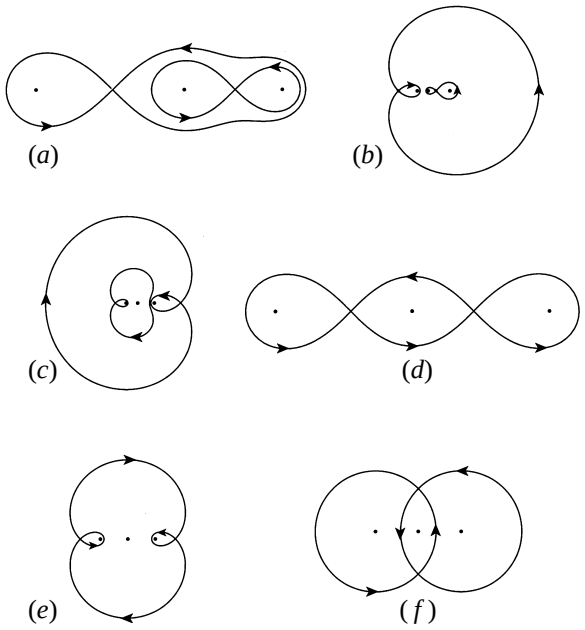

FIGURE 9. Streamline patterns to scale for certain combinations of vortex strengths and positions. In each case vortices are placed on the x-axis. We list the ratio of vortex strengths from left to right, $\Gamma_1:\Gamma_2:\Gamma_3$, the coordinates (x_1, x_2, x_3), and the comparison panel in figure 6: (*a*) 5:3:4, (−3, 0, 2), cf. figure 6(*a*); (*b*) (−1):1:1, (−1, 0, 2), cf. figure 6(*c*); (*c*) 1.8:(−5):2.2, (−1.4, 0, 2), cf. figure 6(*f*); (*d*) 2:1:2, (−1, 0, 1), cf. figure 6(*g*); (*e*) 1:(−3):1, (−1, 0, 1), cf. figure 6(*j*); (*f*) 1:(−1):1, (−1, 0, 1), cf. figure 6(*l*).

start from any two-vortex pattern and 'split' either point vortex into two, as we did in our topological argument. Indeed, it should be possible to produce all the patterns using three vortices restricted to be on a line. In practice, however, if one simply draws the streamline pattern for a set of vortex positions and strengths chosen arbitrarily, some of the patterns in figure 6 are found to arise much more frequently than others. Furthermore, the size of the individual loops makes some of the patterns tedious to compute and plot. For these reasons we are content to show a sampling of patterns to scale in figure 9.

5.2. *Change of streamline topology*

It is natural next to inquire into the possible changes in streamline topology as the motion of the three vortices evolves. This question is of some interest, as we shall see, in providing a deeper understanding of the three-vortex motion itself. The physical importance of a change in streamline topology to processes such as fluid mixing, unfortunately, is not entirely clear, since an instantaneous streamline is not a material curve. A general discussion appears difficult in any event, and we have had to limit ourselves to consideration of the special cases $\Gamma_1 = \Gamma_2 = \pm\Gamma_3$.

For identical vortices, consider the symmetrical configurations in which the vortices form an isosceles triangle. Number the vortices such that vortex 3 is situated on the perpendicular bisector of the side connecting vortices 1 and 2. Then, if 3 is far from 12, the streamline topology must clearly be of the type shown in figure 6(*a*), and both stagnation points will be on the perpendicular bisector of 12 by symmetry. On the other hand, if 3 is on or close to the line 12, the streamline topology must be that of figure 6(*g*), with the stagnation points located symmetrically on either side of the perpendicular bisector of 12. It is clear that for such configurations the streamfunction

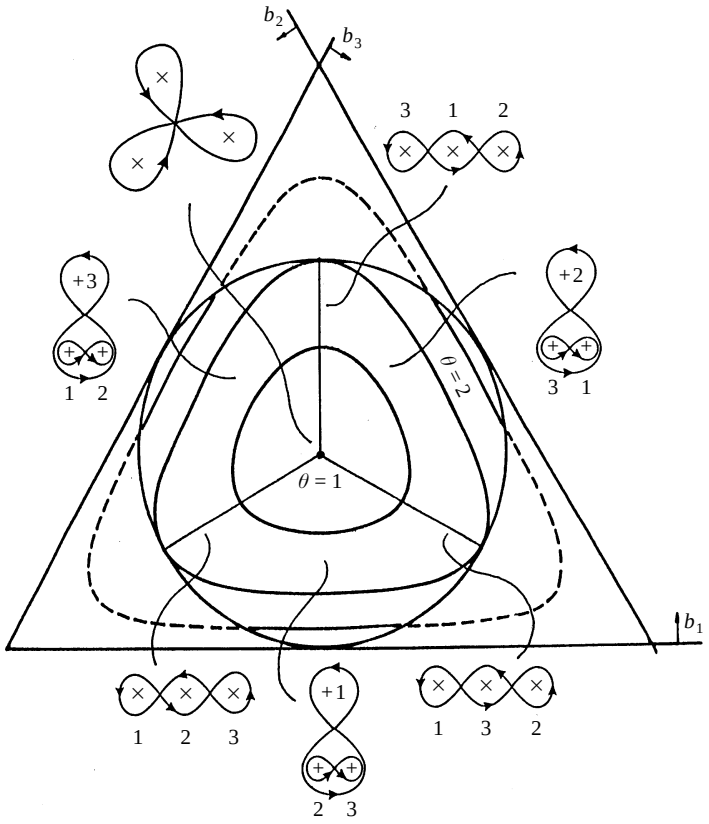

FIGURE 10. 'Phase diagram' for three identical vortices (cf. Aref 1979) with the three bifurcation lines.

assumes the same value at both stagnation points. Thus, considering the family of isosceles triangles that arise as vortex 3 is moved along the perpendicular bisector of 12, we see that there is exactly one point at which the streamline pattern changes from the topology of figure 6(*a*) to that of figure 6(*g*). At this cross-over point the streamline topology is that of figure 7(*a*), which occurs precisely when the vortices form an equilateral triangle.

Now, let us connect these purely kinematical results to the dynamic problem of the motion of three identical vortices. In figure 10 we have reproduced the 'phase diagram' that summarizes the relative motion of the three vortices from Aref (1979, figure 2). The distances of a point in this diagram from the three sides of the equilateral triangle represent the squares of the corresponding sides in the actual vortex triangle. As the vortices move, the 'phase point' either orbits a 'rounded triangle' curve, similar to the special one labelled $\theta = 2$ in figure 10, or oscillates back and forth on the segment of such a rounded triangle that is within the inscribed circle. Because of the triangle inequalities, the only physically accessible region of the diagram in figure 10 is the interior of the inscribed circle (for additional details see Aref 1979). The parameter θ is a measure of the amount of kinetic energy of the motion. The cases $\theta = 1$ and $\theta = 2$ are special. For $\theta = 1$ the vortices form an equilateral triangle that rotates like a rigid body. For $\theta = 2$ the vortices will asymptotically (i.e. as $t \to \infty$) approach a rigidly rotating, collinear configuration.

The three line segments radiating out from the centre of the triangle in figure 10

correspond to isosceles triangle configurations for which the streamline topology is of the type shown in figure 6(*g*): the two equal sides in the isosceles vortex triangle are shorter than the third side. As the vortices move, the 'phase point' in figure 10 will either intersect all three of these radial lines (when $1 < \theta < 2$), or will not intersect any of them (when $\theta > 2$). In the former case, the streamline topology is generally that of figure 6(*a*), but three times per period of the relative motion of the vortices it bifurcates, changing for an instant to that of figure 6(*g*) as the vortices form an obtuse-angled, isosceles triangle, and then returning to the pattern figure 6(*a*) but with two different vortices in the 'figure-eight' streamline loop. In the latter case, the streamline topology is always that of figure 6(*a*), and the same two vortices are surrounded by the 'figure eight' streamline pattern at all times. In figure 10 we have indicated the streamline topology for each region, and numbered the constituent vortices to indicate which one is to be found within which streamline loop.

It is interesting to recall that the orientation of the vortex triangle is invariant in the case $1 < \theta < 2$ (i.e. when the streamline topology undergoes repeated changes), but switches every time the vortices become collinear when $\theta > 2$ (although the streamline topology is invariable)! In the special case $\theta = 1$ the vortices rotate rigidly as an equilateral triangle and the streamline topology is that of the degenerate case in figure 7(*a*). For $\theta = 2$ the streamline topology of the asymptotic, rotating, collinear state is that of figure 6(*g*). During the approach to that state the streamline topology will be as in figure 6(*a*).

The hyperbolic case of three vortices with circulations $\Gamma_1 = \Gamma_2 = -\Gamma_3$ proceeds similarly. *A priori* we might expect to have as possibilities for the instantaneous streamline pattern the cases labelled (*b*), (*c*), (*d*), (*h*), (*i*) and (*l*) in figure 6. However, of these only (*c*) and (*l*) are possible. The reason is that in all the other patterns one can find a closed loop encircling the negative vortex and a positive vortex. This is impossible since the negative vortex exactly cancels either of the positive vortices, and no such closed loop can exist. Now we proceed as above. Consider configurations with all three vortices on a line. If the negative vortex 3 is far away from vortices 1 and 2, the streamline pattern clearly must be of the type in figure 6(*c*) with both stagnation points on the line through the vortices. If 3 is situated somewhere between 1 and 2, we find a streamline pattern with the topology of figure 6(*l*), and stagnation points will be symmetrically positioned above and below the line through the vortices. (These results are consistent with our earlier observation that the stagnation points in this case are on the bisector of $\angle 231$.) We leave it to the reader to elaborate the correspondence with the regimes of motion established in the earlier analysis of this problem (Aref 1979, figure 4).

6. Conclusions and extensions

It is possible to extend the analysis given here to the related problem of the 'atmosphere' of a translating vortex system, i.e. the fluid region carried along by a translating vortex pair, first discussed by Kelvin (1867). In this problem one is again concerned with the number and location of stagnation points in a frame of reference following the vortices, which are in steady translation. It is possible to find a 'Siebeck curve' such that these stagnation points arise as its foci. In the same coordinates as used in §5.1 the equation of this curve is

$$(\Gamma_1\Gamma_2+\Gamma_2\Gamma_3+\Gamma_3\Gamma_1)\,U_1\,U_2\,U_3+(\Gamma_1\,U_1+\Gamma_2\,U_2+\Gamma_3\,U_3)\times(\Gamma_1\,U_2\,U_3+\Gamma_2\,U_3\,U_1+\Gamma_3\,U_1\,U_2)=0. \tag{6.1}$$

This curve is of class 3. It has three distinct, real foci, in general, which are the stagnation points in the co-moving frame.

It is also possible to extend the analysis to the case of vortices in a periodic strip (M. A. Stremler, private communication, 1997). This problem is of interest in conjunction with the dynamics of two-dimensional jets and wakes. The velocity field in a strip of width L is now given by

$$u - \mathrm{i}v = \frac{1}{2L\mathrm{i}} \sum_{\alpha=1}^{N} \Gamma_\alpha \cot\left\{\frac{\pi}{L}(z - z_\alpha)\right\} \tag{6.2}$$

in place of (2.1). Using the addition formula for the cotangent, one finds a stagnation point to correspond to a root of a polynomial in $\tan(\pi z/L)$. The procedures of §§2–4 can now be applied in the conformally mapped plane.

Determining the number, nature and location of stagnation points for a system of point vortices is, clearly, one of the simplest problems of its kind. The stagnation points in this case are the roots of a certain polynomial, and calculating them for a given configuration of vortices of known strengths is, in principle, elementary. A geometrical characterization of the location of stagnation points, and an understanding of how their number and position varies when the strengths and/or positions of the vortices are changed, leads to less familiar mathematical problems and tools, such as the algebraic geometry developed by Plücker and Siebeck a century ago and the use of the complex projective plane. Among the many results obtained the most surprising may be for the case of three vortices of zero net circulation, where a 'similarity law' for the location of the single stagnation point emerged.

The approach of this paper does not appear to be particularly useful if the number of vortices is large, since the order of the polynomial giving Siebeck's curve is then unmanageably large, and the best one can do is probably to determine all stagnation points numerically at every step of the motion. For a small number of vortices, on the other hand, the algebraic-geometric specification of stagnation points presented here is as precise as one can hope to achieve.

The location of stagnation points is intimately connected with the topology of the streamline pattern of the flow induced by the vortices. The possible streamline topologies can be found by the process, illustrated here for three vortices, of assembling such patterns by 'substituting' for a vortex in a pattern with N vortices one of the patterns for two vortices (figure 5) and thus arriving at a streamline pattern for $N+1$ vortices. For some simple choices of the vortex strengths it was possible to describe transitions between different streamline topologies as the vortices move.

We are indebted to Phil Boyland, Slava Meleshko, Mark Stremler, and Anders Thorup for comments and discussion on several aspects of this work. Mark Stremler kindly provided the program used to produce the streamline plots in figure 9. This work was supported by National Science Foundation grant CTS-9311545.

REFERENCES

Aref, H. 1979 Motion of three vortices. *Phys. Fluids* **22**, 393–400.

Aref, H. 1989 Three vortex motion with zero total circulation: Addendum. *Z. Angew. Math. Phys.* **40**, 495–500.

Aref, H. 1992 Trilinear coordinates in fluid mechanics. In *Studies in Turbulence* (ed. T. B. Gatski, S. Sarker & C. G. Speziale), pp. 568–581. Springer.

Aref, H. & Brøns, M. 1995 On stagnation points in vortex flows. *Bull. Am. Phys. Soc.* **40**, 1921.

COXETER, H. S. M. 1993 *The Real Projective Plane*, 3rd Edn. Springer.

ECKHARDT, B. 1988 Integrable four-vortex motion. *Phys. Fluids* **31**, 2796–2801.

ECKHARDT, B. & AREF, H. 1988 Integrable and chaotic motions of four vortices II: Collision dynamics of vortex pairs. *Phil. Trans. R. Soc. Lond.* A **326**, 655–696.

FERRERS, N. M. 1866 *An Elementary Treatise on Tri-linear Coordinates, the Method of Reciprocal Polars and the Theory of Projections*, 2nd Edn. Macmillan.

HEAWOOD, P. J. 1906 Geometrical relations between the roots of $f(x) = 0$ and $f'(x) = 0$. *Q. J. Maths* **38**, 84–107.

KELVIN, LORD 1867 On vortex atoms. *Proc. R. Soc. Edinb.* **6**, 94–105.

LAMB, H. 1932 *Hydrodynamics*, 6th Edn, §154. Cambridge University Press (republished by Dover).

MARDEN, M. 1949 *Geometry of Polynomials*. Am. Math. Soc.

ROTT, N. 1989 Three vortex motion with zero total circulation. *Z. Angew. Math. Phys.* **40**, 473–494.

SALMON, G. 1854 *A Treatise on Conic Sections*, 6th Edn. Chelsea, New York.

SCHOENBERG, I. J. 1982 *Mathematical Time Exposures*. The Mathematical Association of America.

SIEBECK, F. H. 1864 Ueber eine neue analytische Behandlungsweise der Brennpunkte. *J. Reine Angew. Maths* **64**, 175–182.

SYNGE, J. L. 1949 On the motion of three vortices. *Can. J. Maths* **1**, 257–270.